

Praseodymium centers in alkali halides

S. Radhakrishna and B. D. Sharma

Department of Physics, Indian Institute of Technology, Madras, India

(Received 30 July 1973)

Optical and electrical properties of praseodymium-doped NaCl, KCl, RbCl, and KBr crystals are reported. In the optical spectra, both intraconfigurational $f \rightarrow f$ transitions and interconfigurational $f \rightarrow d$ transitions have been observed. An analysis of the $f \rightarrow f$ transitions at 77 and 4.2 °K indicates that each free-ion level of the $4f^2$ configuration splits into $(2J + 1)$ Stark components implying that the symmetry of the crystal field at the ion site is C_2 , or lower. X irradiation produces a small number of divalent praseodymium ions. Ionic-conductivity experiments reveal that the impurity ion is bound to the charge-compensating vacancies by an energy lying in the range 0.6–0.8 eV for the crystals studied. Dielectric-loss experiments give two loss peaks arising owing to the relaxation of impurity-vacancy dipoles at nearest-neighbor (nn) and next-nearest-neighbor (nnn) sites, respectively. This suggests that the trivalent impurity is bound to the two charge-compensating vacancies with vacancies occupying both nn and nnn sites. This results in a C_2 symmetry at the ion site.

I. INTRODUCTION

A considerable amount of work has been done on the nature of divalent impurity centers in alkali-halide crystals.^{1–3} However, only a few stray attempts have been made in the last few decades to get information regarding trivalent impurity centers in alkali-halide crystals.^{4–8} These attempts have met with only partial success, since either the trivalent state of impurity could not be confirmed by independent experiments or both the trivalent and divalent states were invariably present together. It has been shown by Lidiard⁹ that the impurity ion may be present in the alkali-halide matrices in divalent state only if its third ionization potential is greater than 22 eV. A survey of the Periodic Table shows that most of the metals have a third ionization potential greater than 22 eV and they enter the alkali-halide lattices in divalent state only. In the present investigation we have chosen praseodymium to investigate the trivalent impurity centers in alkali halides.

There are two electrons in the $4f$ orbit in trivalent praseodymium ion. When such an ion is placed in a crystal lattice, the f electrons experience a very weak crystal field since they are shielded by the outer $5s^2 6p^6$ electrons. The crystal-field splittings are smaller than the spin-orbit coupling constant. The levels of the $4f^2$ configuration, resulting from L - S coupling, split into their Stark components. The extent to which the $(2J + 1)$ degeneracy is lifted depends on the symmetry of the crystal field.

Transitions between these Stark levels give a number of groups of lines in the absorption spectra. These transitions are parity forbidden but become partially allowed in crystal field owing to mixing of opposite-parity configurations. Such intraconfigurational $f \rightarrow f$ transitions have been studied by

many workers¹⁰ for trivalent praseodymium in several matrices. Some $f \rightarrow f$ transitions have also been reported in KCl and KBr crystals.¹¹ The levels of Pr^{3+} have been established beyond doubt. The $5d$ orbit lies outermost and is strongly affected by the crystal field. The $4f^2 \rightarrow 4f^1 5d^1$ transitions are parity-allowed transitions and are intense.

We have used the optical absorption studies to confirm the trivalent state of praseodymium in the lattices. When such a trivalent impurity enters the alkali-halide crystals by substituting for an alkali ion, two cation vacancies are created for charge compensation. These vacancies carry an effective negative charge and hence are bound to the impurity with electrostatic attraction. Ionic-conductivity experiments yield information regarding the association energy of these impurity-vacancy dipoles. Dielectric-loss experiments have been performed to obtain information regarding the position of the vacancies and the activation energies for the migration of the bound vacancies. Both ionic-conductivity and dielectric-loss results yield considerable information regarding the interaction of impurity with the charge-compensating vacancies.

II. EXPERIMENTAL

Crystals were grown by zone melting and Bridgman techniques in our laboratory. Analytic-reagent-grade BDH alkali-halide powders and E. Merck PrCl_3 powder were used as the starting materials. The crystals were very hygroscopic and therefore were stored carefully in a desiccator. Optical spectra at room, liquid-nitrogen, and liquid-helium temperatures were taken on a Cary-14 spectrophotometer using a metal cryostat. Crystals were quenched from high temperatures before each measurement. X irradiation was done using a Phillips x-ray unit with molybdenum target operating at 35 kV and 15 mA. Both sides of the

crystals were irradiated to get uniform coloration.

Ionic conductivity was measured in vacuum using a megaohm bridge. The temperature was measured by using iron-constantan thermocouple. Both sides of the sample were coated with aquadag to get good electrical contact. The measuring voltage was applied for a short period of time to avoid polarization effects. The readings were taken at different stabilized temperatures and a plot of $\log_{10}\sigma T$ vs $1/T$ was plotted. Dielectric-loss measurements were done using a General Radio 1615A capacitance bridge in combination with a PM-5100 Phillips oscillator. Readings were taken at different frequencies in the frequency range 10^2 – 10^5 Hz at various constant temperatures. The temperature of the crystal was kept constant by using a plastomatic Phillips temperature controller. Plots of $\log_{10}\tan\delta$ (loss factor) vs $\log_{10}f$ (frequency) were plotted at various temperatures. The dielectric-loss mount used in the present investigation is described elsewhere.¹²

III. RESULTS AND DISCUSSIONS

A. Optical properties

1. Uncolored crystals

The optical spectrum of the praseodymium-doped alkali-halide crystals consists of a number of groups of weak and sharp lines in the infrared and visible regions and some broad intense bands in the ultraviolet region. The sharp lines arise owing to the parity-forbidden intraconfigurational ($f \rightarrow f$)

transitions, while the intense bands arise owing to parity-allowed interconfigurational ($f \rightarrow d$) transitions. Both the transitions have been observed and are discussed separately in the following sections.

(a) *Intraconfigurational $f \rightarrow f$ transitions.* Figures 1(a) and 1(b) show the optical spectra of RbCl:Pr³⁺ crystals at 77 and 4.2 °K, respectively, in the wavelength range 440–500 nm. The spectra in the range 580–620 nm is shown in Fig. 2. The spectra consist of groups of sharp lines around 440 nm ($^3H_4 \rightarrow ^3P_2$); 470 nm ($^3H_4 \rightarrow ^3P_1$); 490 nm ($^3H_4 \rightarrow ^3P_0$); 600 nm ($^3H_4 \rightarrow ^1D_2$). All the transitions observed arise from the lowest free-ion manifold 3H_4 to the various levels of the $4f^2$ configuration. This is to be expected since the next higher manifold 3H_5 above the ground manifold is separated by ~ 2000 cm^{-1} from it. Since each free-ion level splits into its Stark levels owing to the symmetry of the crystal field, transitions take place from the various Stark levels of the ground manifold 3H_4 to the Stark components of the other free-ion levels. The number of lines is greatly reduced at 4.2 °K, since the higher Stark levels of the ground manifold 3H_4 are depopulated. The position of all the lines observed are tabulated in Table I for NaCl, KCl, RbCl, and KBr crystals. An analysis of the spectra at 300, 77, and 4.2 °K shows that each free-ion level splits into $(2J+1)$ Stark components and the J degeneracy is completely lifted. This indicates that the site symmetry at the ion has at most a twofold axis. Efforts to study polarization spectra did not succeed in the usual sense to help the identification of vari-

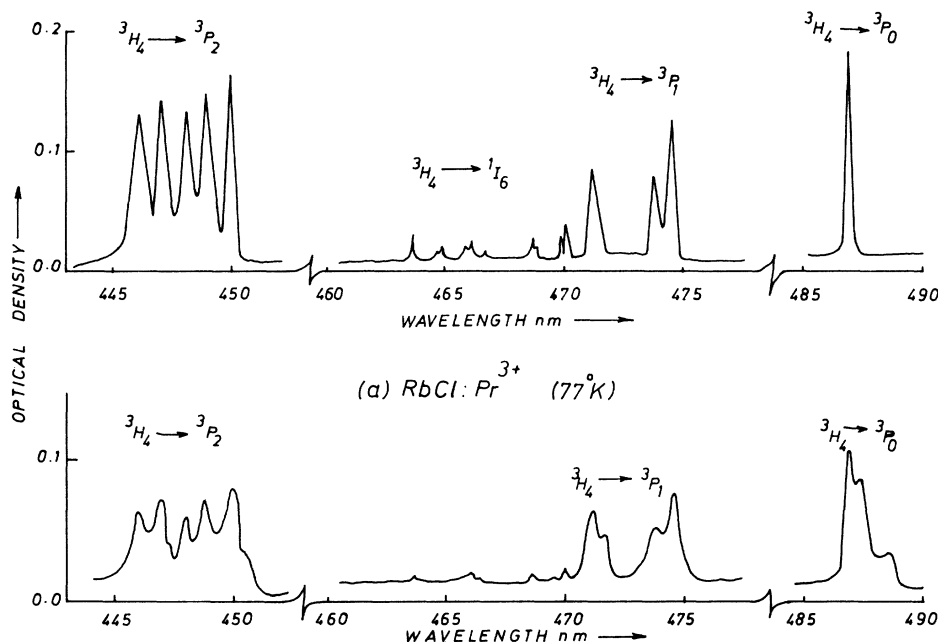


FIG. 1. Optical absorption spectra of Pr³⁺-doped RbCl crystals at 77 and 4.2 °K.

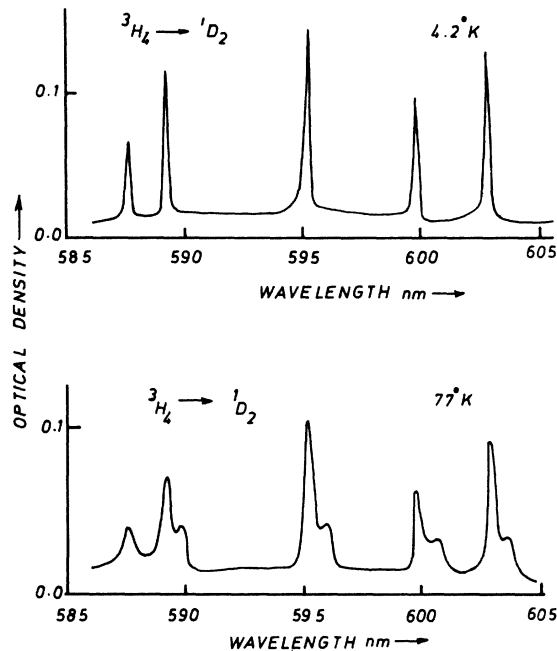


FIG. 2. ${}^3H_4 \rightarrow {}^1D_2$ transition of Pr^{3+} in RbCl crystals at 77 and 4.2°K.

ous transitions and the site symmetry.

The simplest group of lines corresponds to the transition ${}^3H_4 \rightarrow {}^3P_0$. At 4.2°K only one line is observed while three lines are observed in this transition at 77°K. Since 3P_0 is nondegenerate state, these transitions take place from the Stark levels of the ground manifold 3H_4 . Nine lines are observed in this transition at 300°K. This indicates that 3H_4 has split into nine levels. Thus the nine Stark levels of the ground manifold and the position of 3P_0 level are directly obtained from this transition. The transition near 470 nm corresponds to ${}^3H_4 \rightarrow {}^3P_1$. Four or five lines are obtained in this transition at 77°K. At 4.2°K, there are only three lines which are attributed to the transitions from the lowest Stark component of the ground manifold to the three Stark components of the 3P_1 level. The transition near 440 nm corresponds to ${}^3H_4 \rightarrow {}^3P_2$. Only five lines are observed at 4.2°K in this group of lines. At 77°K few more lines are added to the spectrum. These additional lines are well identified in other crystals (where liquid-helium spectra were not available) from the simple fact that they lie on the low-energy side of the main lines separated by an energy equal to the difference between the two lowest Stark components of the ground manifold. A similar transition ${}^3H_4 \rightarrow {}^1D_2$ is observed around 600 nm. In this transition ten lines are observed at 77°K and five lines are observed at 4.2°K. This indicates that 3P_2 and 1D_2 levels split into five Stark components each.

1I_6 and 1G_4 levels are partially observed and are very weak in intensity. The 1S_0 level, however, is not observed at all. It lies near 200 nm, where it is possibly obscured by the intense $f \rightarrow d$ transitions. 3F_3 and 3F_4 levels consist of a number of diffused lines but are quite intense. There might be a possibility of overlapping. The centers of gravity of these levels could not be determined from the available absorption spectra. Eight lines are observed in the transition ${}^3H_4 \rightarrow {}^3F_2$ near 2000 nm. All the five Stark components of this level are determined from the absorption spectra. 3H_5 and 3H_6 levels were not investigated since they lie in the far infrared. The positions of the various Stark components of the levels of Pr^{3+} observed are tabulated in Table II along with the levels in $LaCl_3 \cdot Pr^{3+}$ crystal¹³ for a comparison.

The transitions to the levels 3P_2 , 3P_1 , and 3P_0 from the ground manifold are schematically shown

TABLE I. Positions in (cm^{-1}) of various lines observed in $f \rightarrow f$ transitions of Pr^{3+} ion in different crystals at 77°K.

| Transitions | Crystals | | | |
|-------------------------------|----------|--------|--------|--------|
| | NaCl | KCl | RbCl | KBr |
| ${}^3F_2 \rightarrow {}^3H_4$ | 4990 | 5003 | 4986 | 4960 |
| | 4999 | 5040 | 5007 | 4982 |
| | 5030 | 5047 | 5050 | 5003 |
| | 5063 | 5058 | 5056 | 5020 |
| | 5074 | 5080 | 5062 | 5030 |
| | 5084 | 5106 | 5079 | 5054 |
| | 5100 | | 5100 | |
| ${}^3H_4 \rightarrow {}^1D_2$ | 16 544 | 16 552 | 16 563 | 16 515 |
| | 16 552 | 16 561 | 16 584 | 16 527 |
| | 16 655 | 16 655 | 16 644 | 16 607 |
| | 16 757 | 16 664 | 16 667 | 16 621 |
| | 16 765 | 16 787 | 16 774 | 16 716 |
| | 16 946 | 16 950 | 16 796 | 16 729 |
| | 16 954 | 16 960 | 16 945 | 16 868 |
| | 16 992 | 17 001 | 16 965 | 16 905 |
| | 17 000 | 17 010 | 17 014 | 16 197 |
| | | | | |
| ${}^3H_4 \rightarrow {}^3P_0$ | 20 446 | 20 446 | 20 463 | 20 370 |
| | 20 490 | 20 505 | 20 510 | 20 406 |
| | 20 498 | 20 514 | 20 531 | 20 418 |
| ${}^3H_4 \rightarrow {}^3P_1$ | 21 036 | 21 047 | 21 072 | 20 956 |
| | 21 045 | 21 056 | 21 102 | 20 967 |
| | 21 064 | 21 074 | 21 192 | 21 000 |
| | 21 189 | 21 194 | 21 216 | 21 099 |
| | 21 197 | 21 203 | | |
| ${}^3H_4 \rightarrow {}^3P_2$ | 22 188 | 22 194 | 22 200 | 22 110 |
| | 22 197 | 22 205 | 22 220 | 22 122 |
| | 22 242 | 22 283 | 22 274 | 22 196 |
| | 22 250 | 22 347 | 22 309 | 22 254 |
| | 22 331 | 22 356 | 22 345 | 22 266 |
| | 22 363 | 22 380 | 22 366 | 22 285 |
| | 22 371 | 22 403 | 22 413 | 22 310 |
| | 22 407 | 22 412 | | |
| | | | | |
| | | | | |

TABLE II. Position (in cm^{-1}) of Stark splits of various levels of praseodymium ion in alkali-halide crystals. Values in parentheses indicate the Stark splitting of the level.

| Level | NaCl | KCl | RbCl | KBr | LaCl ₃ (Ref. 10) |
|-----------------------------|--------|--------|--------|--------|--------------------------------|
| ³ H ₄ | 0 | 0 | 0 | 0 | 0 |
| | 8 | 8 | 21 | 12 | 33 |
| | 53 | 66 | 69 | 48 | 96 |
| | 126 | 120 | 120 | 96 | 130 |
| | 145 | 157 | 163 | 138 | 137 |
| | 237 | 235 | 240 | 205 | 199 |
| | 342 | 350 | 356 | 290 | |
| | 431 | 440 | 438 | 410 | |
| | 520 | 518 | 510 | 483 | |
| ³ F ₂ | 4990 | 5003 | 5007 | 4960 | 4922 |
| | 5030 | 5040 | 5050 | 4982 | 4950 |
| | 5063 | 5058 | 5062 | 5003 | |
| | 5084 | 5080 | 5079 | 5030 | |
| | 5100 | 5106 | 5100 | 5054 | |
| | (110) | (103) | (93) | (94) | (28) |
| ¹ D ₂ | 16 552 | 16 567 | 16 584 | 16 527 | 16 630 |
| | 16 655 | 16 660 | 16 667 | 16 621 | 16 670 |
| | 16 765 | 16 785 | 16 796 | 16 729 | 16 780 |
| | 16 954 | 16 960 | 16 965 | 16 868 | |
| | 17 000 | 17 010 | 17 014 | 16 917 | |
| | (448) | (443) | (430) | (390) | (150) |
| ³ P ₀ | 20 498 | 20 514 | 20 531 | 20 418 | 20 474 |
| ³ P ₁ | 21 045 | 21 056 | 21 072 | 20 967 | 21 066 |
| | 21 064 | 21 056 | 21 102 | 21 000 | 21 096 |
| | 21 197 | 21 203 | 21 216 | 21 099 | |
| | (152) | (147) | (144) | (132) | (30) |
| ³ P ₂ | 22 196 | 22 205 | 22 220 | 22 122 | 22 207 |
| | 22 250 | 22 283 | 22 274 | 22 196 | 22 226 |
| | 22 331 | 22 356 | 22 309 | 22 266 | 22 246 |
| | 22 371 | 22 380 | 22 366 | 22 285 | |
| | 22 407 | 22 412 | 22 413 | 22 310 | |
| | (211) | (207) | (193) | (188) | (39) |

in Fig. 3. It can be seen from Table II that while the J degeneracy is completely lifted in alkali-halide matrices, it is partially lifted in LaCl₃ crystals. Also the Stark splittings are larger in alkali halides than in LaCl₃ crystals. This is schematically shown in Fig. 4. This shows that the Pr³⁺ ions experience a stronger field in alkali halides than in LaCl₃. Table III summarizes the centers of gravity (cg) of the various manifolds (the cg of the ground manifold ³H₄ taken as the zero-level reference of energy). It can be seen that the levels in KBr lie lower in energy than in KCl. This may be attributed to the larger size of bromine which results in a smaller Coulomb interaction between the two f electrons.

The energies of various free-ion levels are described¹⁰ in terms of Slater integrals F_k and spin-orbit coupling constant ξ . In case of f electrons

only F_2 , F_4 , F_6 , and ξ may be considered. These parameters have small dependence on the crystal field, and thus can be calculated by Taylor-series expansion as suggested by Wong.¹⁴ The Taylor-series expansion of the energy of a level j is given by

$$E_j = E_j^0 + \sum_{i=1}^4 \frac{\partial E_j}{\partial P_i} \Delta P_i,$$

where E_j is the energy of a level j , E_j^0 is the zero-order energy of level j and P_i are the parameters. The data on the levels ³P₂, ³P₁, ³P₀, ¹D₂, and ³F₂ have been used to calculate these parameters in the present case. The zero-point energy and the various partial derivatives have been taken from earlier data¹⁵ on LaCl₃:Pr³⁺ system where configurational interactions were also taken into account. The value of F_2 , F_4 , F_6 , and ξ thus calculated using a least-squares-fitting procedure are tabulated in Table III along with the calculated centers of gravity of the levels using these parameters. However, since only a few of the levels could be obtained, these parameters could not be determined to the best fit. From these $f \rightarrow f$ transitions it is evident that praseodymium exists in its trivalent state.

(b) *Interconfigurational $f \rightarrow d$ transitions.* Intense bands are observed in the uv region of the spectrum. Figure 5 shows the spectra of RbCl:Pr³⁺ crystals at 300 and 77°K. Two bands are observed at 231 and 202 nm at 300°K. These bands are attributed to the parity-allowed $4f \rightarrow 5d$ transitions. Such $f \rightarrow d$ transitions have been reported¹⁸ in the case of CaF₂ crystals doped with trivalent praseodymium. Since the $5d$ orbitals lie outermost, they experience a strong crystal field. In an octahedral environment, the d orbitals will split into t_2 and e levels. It is found that the crystal-field splittings¹⁶ in rare-earth ions are $\sim 10^4$ cm^{-1} . The approximation that the states of $4f^1 5d^1$ configuration behave as those of a single electron in the d shell, which splits into t_2 and e orbitals, slightly perturbed by the $4f^1$ core electrons, holds good.^{16,17} The system becomes much simpler since only one d electron is involved. Since in the present case, the symmetry is still lower, the t_2 and e levels further split into a total of five orbitals. Transitions from the ground state of $4f^2$ configuration to each of these five orbitals should be observed. However, in the present case, the fundamental absorption of the host crystals starts around 180 nm and only two of such $f \rightarrow d$ transitions could be observed. The two transitions thus observed are attributed to the transitions from the ground state ³H₄ of the $4f^2$ configuration to the two lowest components of the d orbit.

The peak positions and half-widths of these bands are tabulated in Table IV, both at 77 and 300°K. These bands sharpen and shift to the low-energy

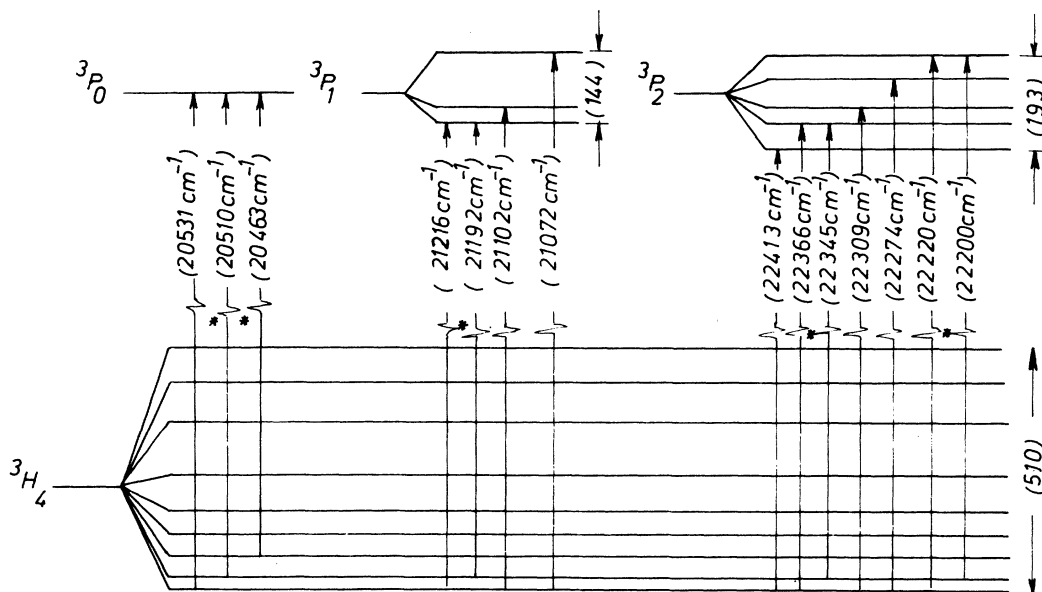


FIG. 3. Transitions from 3H_4 to 3P_0 , 3P_1 , and 3P_2 levels of praseodymium in RbCl crystals observed at 77°K. Transitions marked (*) disappear as the temperature of measurement is lowered to 4.2°K. All values are in cm $^{-1}$ (vacuum).

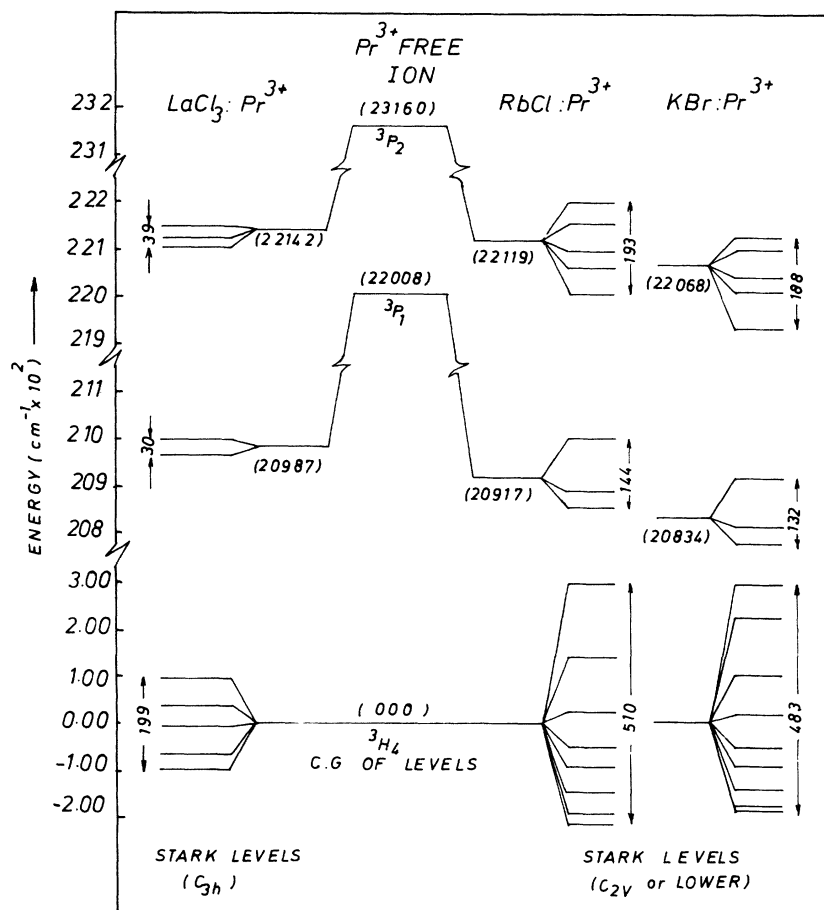


FIG. 4. Effect of crystal field on free-ion values of Pr $^{3+}$ (values in cm $^{-1}$).

TABLE III. Observed and calculated centers of gravity for some levels of Pr^{3+} in various alkali-halide matrices. All values are in cm^{-1} (vacuum). Values in parentheses indicate the calculated values for the levels using F_2 , F_4 , F_6 , and ξ .

| Level | NaCl | KCl | RbCl | KBr | Free ion (Ref. 10) |
|------------|--------------------|--------------------|--------------------|--------------------|-----------------------|
| 3H_4 | 0 | 0 | 0 | 0 | 0 |
| 3F_2 | 4846 (4820) | 4845 (4819) | 4847 (4823) | 4833 (4803) | 4997 |
| 1D_2 | 16 579 (16 585) | 16 584 (16 612) | 16 593 (16 598) | 16 544 (16 552) | 17 334 |
| 3P_0 | 20 291 (20 286) | 20 302 (20 298) | 20 318 (20 313) | 20 230 (20 224) | 21 389 |
| 3P_1 | 20 892 (20 945) | 20 899 (20 952) | 20 917 (20 965) | 20 834 (20 895) | 22 007 |
| 3P_2 | 22 104 (22 056) | 22 113 (22 024) | 22 119 (22 075) | 22 068 (22 013) | 23 160 |
| Parameters | | | | | |
| F_2 | 307.21 | 307.43 | 307.69 | 306.15 | |
| F_4 | 21.20 | 20.53 | 20.65 | 18.35 | |
| F_6 | 2.814 | 1.905 | 1.921 | 2.757 | |
| ξ | 721.16 | 720.91 | 719.73 | 725.75 | |

side at lower temperatures. The shift is attributed to the increase in crystal field caused due to the contraction of lattice. The half-width of these bands in the present case is found to be $\sim 2500 \text{ cm}^{-1}$, which is large compared to the half-width ($\sim 1700 \text{ cm}^{-1}$) reported in CaF_2 crystals.¹⁶ The lowest $4f \rightarrow 5d$ transition observed¹⁸ in a free Pr^{3+} gas ion is around $61\,000 \text{ cm}^{-1}$. Jørgensen¹⁹ has also given a theoretical formula to estimate the position of lowest $4f \rightarrow 5d$ transitions of rare-earth ions. The lowest transition observed in the alkali halides is around $40\,000 \text{ cm}^{-1}$. Thus in alkali halides there is a lowering of $\sim 21\,000 \text{ cm}^{-1}$ in the energy of the lowest $4f \rightarrow 5d$ transition from the corresponding free-ion lowest $4f \rightarrow 5d$ transition. This is attributed to the crystal-field lowering of the ground state of $4f^1 5d^1$ configuration. Since only two of the transitions could be observed, the value of $10Dq$ (crystal-field strength) could not be estimated.

No vibronic structure could be observed in these $f \rightarrow d$ bands as reported in the case of CaF_2 crystals.¹⁶ It is found¹⁶ that in some cases, this vibronic nature of the band is masked away by strains of unknown origin. No cluster formation was observed in lightly ($\sim 50 \text{ ppm}$) doped crystals quenched from high temperatures. However, on storing for a long time or in heavily doped samples, a broad absorption started near 240 nm partially masking the $f \rightarrow d$ bands. This additional absorption may be due to the cluster formation of Pr^{3+} ions, as has been observed in CaF_2 crystals.¹⁶ All the measurements were, therefore, performed on crystals freshly quenched from high temperatures.

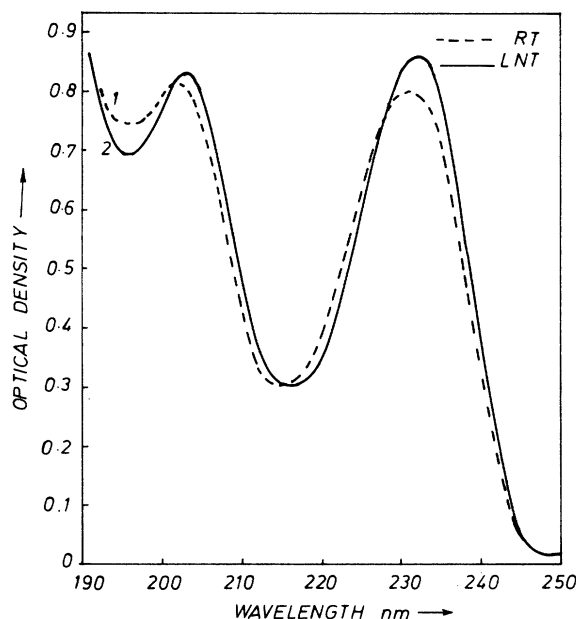


FIG. 5. Optical absorption spectra of $\text{RbCl}:\text{Pr}^{3+}$ at 300°K (curve 1) and 77°K (curve 2).

2. Colored crystals

In order to study the effect of ionizing radiations on the valence state of the Pr^{3+} ion, some x-irradiation experiments were performed. Thin crystals containing $50\text{--}100\text{-ppm}$ Pr^{3+} were used. Since $f \rightarrow f$ transitions are too weak in intensity, attention was focused on the strong $f \rightarrow d$ transitions. Figure 6 shows the optical spectra of $\text{KCl}:\text{Pr}^{3+}$ crystals before and after x irradiation. A slight decrease in the intensity of $f \rightarrow d$ bands is observed. Many weak bands, in addition to the F band formed at 556 nm , make their appearance in the visible and infrared regions. These bands cause a small

TABLE IV. Peak positions (nm) and half-width (eV) of various $f \rightarrow d$ transitions in Pr^{3+} -doped crystals at 300 and 77°K .

| Crystal | Peak position (nm) | | Half-width on low-energy side (eV) | |
|---------|---------------------|--------------------|------------------------------------|--------------------|
| | 300°K | 77°K | 300°K | 77°K |
| NaCl | 239 | 241 | 0.31 | 0.30 |
| | 212 | 213 | | |
| KCl | 238 | 240 | 0.30 | 0.29 |
| | 210 | 211 | | |
| RbCl | 231 | 232 | 0.32 | 0.31 |
| | 202 | 203 | | |
| KBr | 271 | 273 | 0.26 | 0.25 |
| | 234 | 235 | | |

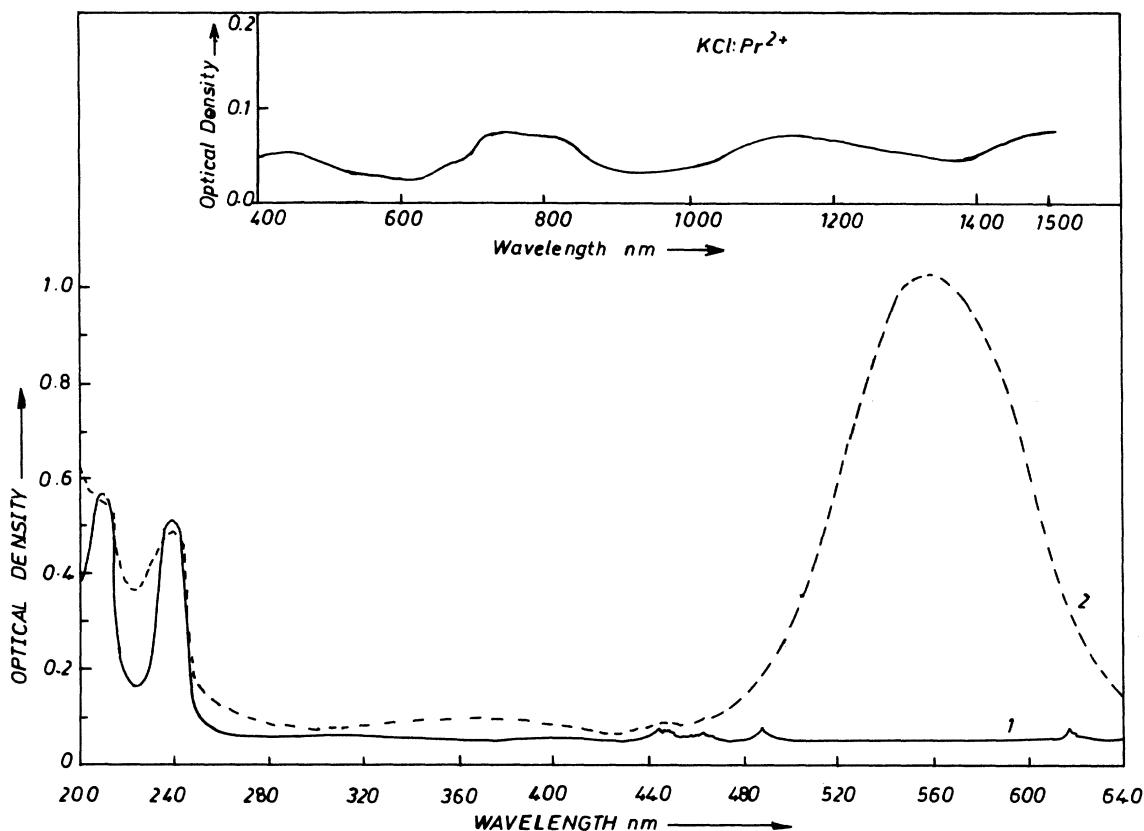


FIG. 6. Optical absorption spectra of KCl crystals containing 80 ppm of Pr^{3+} . Curves 1 and 2 are obtained before and after x irradiation at room temperature. The inset shows the additional spectra which appears after x irradiation.

broadening of the F band. However, the half-width of F band is nearly the same as obtained in pure crystals. The inset in Fig. 6 shows the spectrum which appears after x irradiation. It consists of many broad and weak bands. The decrease in intensity of $f \rightarrow d$ bands of Pr^{3+} indicates a change in the valence state of Pr^{3+} ions. In case the valency has changed to Pr^{4+} one should observe some $f \rightarrow f$ transitions in the visible and infrared regions. However, since broad bands are observed in the visible and infrared regions, it indicates a change of valence state to Pr^{2+} . The $4f^2 5d^1$ and $4f^3$ configurations¹⁰ of Pr^{2+} lie well below $50\,000\text{ cm}^{-1}$ and a large number of them overlap. In a crystal field, the $4f^2 5d^1$ configuration is further lowered in energy. All the transitions from the ground state of $4f^3$ configurations to the various $4f^1 5d^1$ levels are parity allowed and therefore should be observed in the optical spectrum. A similar case of reduction of Pr^{3+} to divalent state has been reported¹⁷ for γ -irradiated CaF_2 crystals. Similar broad bands were observed. The ground state of Pr^{2+} is determined by the ground state of the $4f^3$ configuration. The spectra becomes complicated due to a large

mixing of $4f^3$ and $4f^2 5d^1$ configurations and the crystal-field splittings of the $5d$ orbit. No transitions corresponding to $f \rightarrow f$ absorption of Pr^{2+} could be observed possibly because the concentration of Pr^{2+} was very small. Even the intensity of broad bands arising owing to $f \rightarrow d$ transitions of Pr^{2+} were extremely weak. Further irradiation did not produce any new results except the growth of F band.

B. Transport properties

1. Ionic conductivity

Figure 7 shows the ionic conductivity plot ($\log_{10}\sigma T$ vs $1/T$) for $\text{RbCl}:\text{Pr}^{3+}$ crystals. Three regions with slopes 1.97, 0.81, and 1.16 eV are obtained. Interpreting these results on the basis of association model,⁹ the values of different parameters, W_s (energy of Schottky-defect formation), E_c (activation energy for migration of a cation vacancy), and W_a (association energy of the impurity-vacancy pair) are obtained as 2.32, 0.81, and 0.70 eV, respectively. The values of W_s and E_c agree well with the experimental values reported for pure and divalent impurity-doped crystals.²⁰ Similar results

TABLE V. Energy parameters for Pr^{3+} -doped alkali halides obtained from conductivity results: W_s is the energy of formation of Schottky defects; E_c is the energy of migration of cation vacancies; W_a is the free energy of association of the impurity ion and cation vacancies. (All energies are expressed in eV.)

| Crystal | W_s | E_c | W_a |
|---------|-------|-------|-------|
| NaCl | 2.32 | 0.72 | 0.76 |
| KCl | 2.22 | 0.70 | 0.82 |
| RbCl | 2.32 | 0.81 | 0.70 |
| KBr | 2.24 | 0.66 | 0.68 |

are obtained for other alkali-halide crystals and the values of parameters obtained are given in Table V.

It can be seen from Fig. 7 that the association region extends to very high temperatures. This is because of large association energy of the I - V complex. Moreover, the entire association region has only one slope. This indicates that both the vacancies created for charge compensation are bound to the impurity with equal energy and that the absence of one of the two vacancies does not make significant difference to the association energy. This indicates that the vacancies are distributed such that they have minimum interactions. However, nothing can be said about the position of vacancies by conductivity experiments. Earlier results on divalent impurities indicate that the association energy lies in the range 0.3–0.5 eV. Table VI contains the values of W_a obtained by several workers for divalent and trivalent impurities for comparison. It can be seen from Table V that in the present case the value of W_a varies between 0.6 and 0.8 eV. This increase in value of W_a apparently arises owing to the two extra positive charges on the impurity atom, which effectively increase the Coulomb attraction between the impurity and oppositely charged vacancies. This is only an *a priori* explanation and more theoretical work is called for.

Earlier experiments^{4,7} on diffusion of trivalent impurities in alkali halides showed that the diffusion coefficient was independent of impurity concentration. Since impurity-vacancy pairs are formed and their number is governed by law of mass action, the diffusion coefficient is dependent on concentration.⁹ However, the diffusion coefficient may become independent of concentration (a) at very high impurity concentration or (b) when the association energy of impurity-vacancy pair is very large.

Since the experiments⁷ were done at very low concentrations, it was concluded that the association energy was very large. However, the order of energy was not estimated. Recently, some ionic conductivity results⁸ on NaCl crystals containing

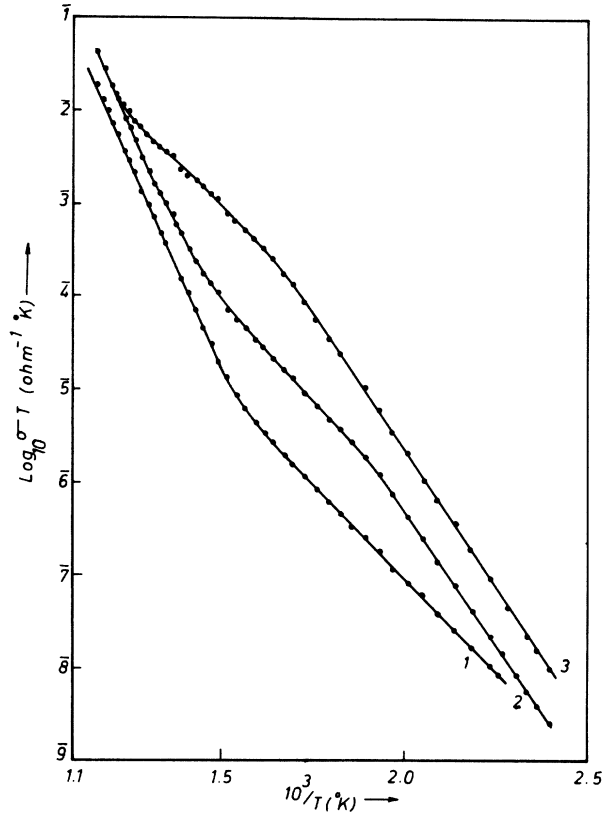


FIG. 7. Conductivity plot for pure and praseodymium-doped RbCl crystals. Curve (1) pure; (2) 25 ppm; and (3) 35 ppm.

Sb^{2+} and a small concentration of Sb^{3+} simultaneously, have yielded the value of $W_a \sim 0.56$ eV. In the same crystal when only Sb^{2+} was present, the value of W_a was found to be ~ 0.3 eV. This indicates that W_a for Sb^{3+} is higher than 0.56 eV, but an accurate value could not be determined since Sb^{2+} was present also. In the present experiments, we have used the lower portions of zone-melt grown crystals to reduce the effect of background divalent im-

TABLE VI. Association energy for various impurities doped in alkali-halide crystals obtained from conductivity results. (All energies are expressed in eV.)

| Crystal | Impurity ion | W_a | Reference |
|---------|----------------------------------|-------|--------------|
| NaCl | Ni^{2+} | 0.32 | 20 |
| NaCl | Co^{2+} | 0.30 | 20 |
| NaCl | Sb^{2+} | 0.30 | 8 |
| NaCl | $\text{Sb}^{2+}, \text{Sb}^{3+}$ | 0.56 | 8 |
| NaCl | Pr^{3+} | 0.78 | Present work |
| KCl | Sr^{2+} | 0.42 | 21 |
| KCl | Cd^{2+} | 0.51 | 21 |
| KCl | Pr^{3+} | 0.72 | Present work |

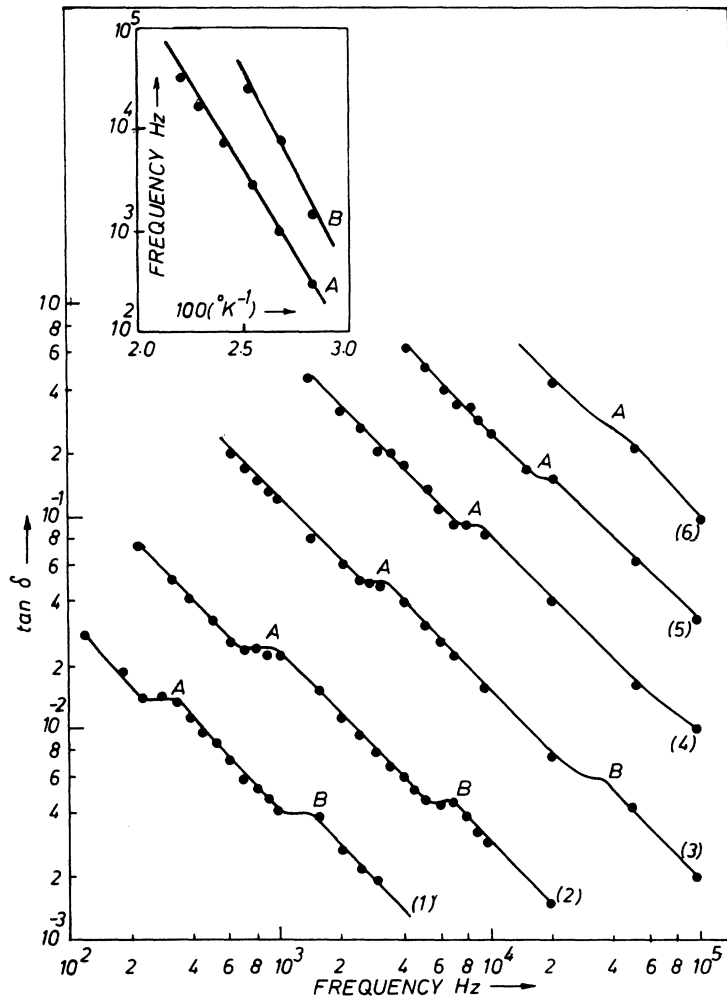


FIG. 8. Dielectric-loss results for NaCl crystal containing 30 ppm of Pr^{3+} . Curves 1, 2, 3, 4, 5, and 6 are obtained at temperatures 80, 100, 120, 140, 160, and 180 °C, respectively. The inset shows the plot of $\log f_m$ vs $1000/T$ for the determination of activation energy and frequency factor.

purities. The background impurities were well below 5 ppm, while the concentration of Pr^{3+} was typically ~ 20 – 50 ppm in different samples. The values of W_a obtained from different samples agreed well within experimental error. Thus it can be concluded that trivalent impurity is more tightly bound to the vacancy than a divalent impurity with the value of W_a lying in the range 0.6–0.8 eV.

2. Dielectric loss

Figure 8 shows the dielectric-loss results ($\tan \delta$ vs f) for NaCl: Pr^{3+} crystals. It can be seen that two loss peaks are obtained. Curves 1–6 are obtained by taking measurements at various constant temperatures. The low- and high-frequency peaks are labeled A and B, respectively. The inset in the figure shows the plot of $\log_{10} f_m$ vs $1/T$ (f_m being the frequency at the maxima of loss peak) for the two peaks. Two straight lines with slopes 0.88 and 0.68 eV are obtained corresponding to the two peaks A and B, respectively. This shows that the peak frequencies obey the Arrhenius relation and

can be expressed as

$$f_{m,A,B} = f_{0,A,B} e^{-E_{A,B}/RT},$$

where f_{mA} and f_{mB} are the peak frequencies; f_{0A} and f_{0B} are the corresponding preexponential factors; E_A and E_B are the activation energies for the two peaks A and B, respectively. Experiments on pure crystals resulted in straight lines with unit slope in $\log_{10} \tan \delta$ vs f plots. To confirm that the peaks were not due to Maxwell-Wagner losses which arise owing to minute air gaps between the electrodes and the sample,²² experiments were performed with different concentration of impurities. A change in height of the two peaks indicated that these peaks were due to the relaxation of trivalent praseodymium impurity-vacancy dipoles. Similar results were obtained with other crystals and the values of different parameters are given in Table VII. Some results as obtained for divalent impurities are also included for comparison.

The vacancies can occupy both the nearest-neighbor (nn) or next-nearest-neighbor (nnn) sites, de-

TABLE VII. Activation energy and frequency factors for *A* and *B* loss peaks for different crystals.

| Crystals | Activation energy (eV) | | Frequency factor f_0 (sec ⁻¹) | | Reference |
|------------------------|------------------------|----------|---|-----------------------|--------------|
| | <i>A</i> | <i>B</i> | <i>A</i> | <i>B</i> | |
| NaCl: Pr ³⁺ | 0.68 | 0.88 | 1.33×10^{12} | 4.49×10^{15} | Present work |
| KCl: Pr ³⁺ | 0.66 | 0.86 | 1.83×10^{10} | 4.20×10^{13} | Present work |
| RbCl: Pr ³⁺ | 0.72 | 0.86 | 5.31×10^{10} | 2.43×10^{13} | Present work |
| KBr: Pr ³⁺ | 0.66 | 0.76 | 1.82×10^{11} | 8.71×10^{12} | Present work |
| NaCl: Co ²⁺ | 0.67 | 0.72 | 3.7×10^{12} | 7.80×10^{13} | 30 |
| NaCl: Ni ²⁺ | 0.62 | 0.55 | 3.69×10^{11} | 2.84×10^{11} | 31 |

pending on the binding energy. It has been shown theoretically^{23,24} that the binding energy of an impurity-vacancy pair with vacancy at nn or nnn site is approximately equal and the difference between the two is ~ 0.04 eV. The presence of a polarizable halogen ion between the impurity and the vacancy at the nnn site compensates for the loss in electrostatic energy due to the increase in the distance of the nnn site from that of the nn site. Thus the vacancy can occupy either of the nn or nnn sites. EPR experiments²⁵ on NaCl: Mn²⁺ and KCl: Mn²⁺ systems have indicated that the vacancies exist both at nn and nnn sites. If the vacancies are present both at nn and nnn sites, the polarization of I-V dipoles can be separated into two discrete relaxation modes.²⁶⁻²⁸ The two relaxation times T_1 and T_2 are given in terms of frequencies W_1 , W_2 , W_3 , and W_4 for the jumps $nn \rightarrow nn$, impurity $\rightarrow nn$, $nnn \rightarrow nn$, and $nn \rightarrow nnn$, respectively, by the expressions

$$1/T_1 = 2W_3 + W_0 + W_4 + [(W_0 + W_4 - 2W_3)^2 + 4W_3W_4]^{1/2}$$

and

$$1/T_2 = 2W_3 + W_0 + W_4 - [(W_0 + W_4 - 2W_3)^2 + 4W_3W_4]^{1/2},$$

where $W_0 = W_1 + W_2$.

Thus two loss peaks should be observed corresponding to the two relaxation times T_1 and T_2 . Such peaks have been reported for many divalent impurities.²⁹⁻³³ In the present case two vacancies are present with each impurity atom. The number of peaks will depend on the relative position of these vacancies.

The jump activation energies of the two peaks *A* and *B* in NaCl: Pr³⁺ are 0.68 and 0.88 eV, respectively. These values compare well with the value obtained from ionic conductivity experiments, which is 0.72 eV. We assign therefore the two loss peaks *A* and *B* to the relaxation of impurity-vacancy dipoles at nnn and nn sites, respectively. The difference between the values of E_A and E_B may arise because of interaction of nn and nnn site vacancies during the reorientations. However, similar differences have been observed in

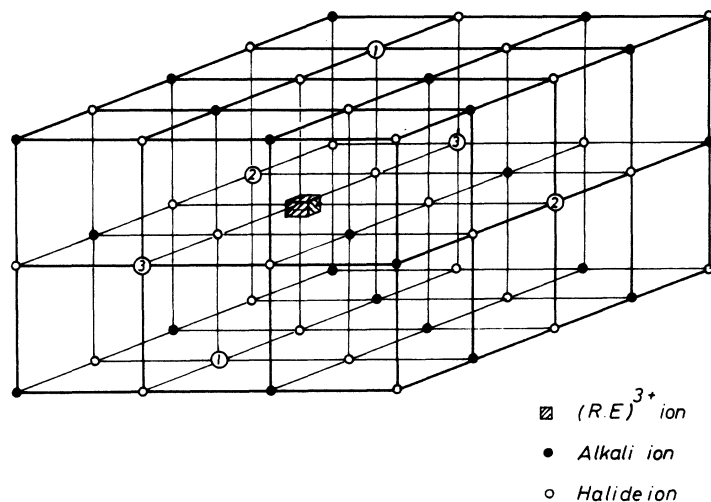


FIG. 9. Trivalent ion in an alkali-halide matrix associated with two cation vacancies in the nearest or next-nearest positions. The three probable site symmetries, namely, D_{2h} , C_s , and D_{4h} are shown by the vacancy pairs labeled 1, 2, and 3, respectively.

the case of divalent impurities also.³⁰⁻³³ The diffusion experiments⁴⁻⁷ indicate that the activation energy for migration of a trivalent impurity ion is $\sim 1.1-1.2$ eV. Thus the activation energies obtained in the present case rule out the possibility of impurity-vacancy jump W_2 and so loss under the B peak arises mainly owing to the jump frequency W_1 for (nn- \bar{nn}) jumps. Thus the dielectric-loss results suggest that the two vacancies occupy both nn and nnn sites.

In the case of a trivalent impurity, the two charge compensating vacancies can be accommodated in a number of ways. However, since both the cation vacancies have similar charge, they will repel each other. Thus the positions where these vacancies lie close to each other will not be favored according to energy considerations. Excluding such possibilities there are three different ways in which the vacancies can exist with minimum interactions (ionic conductivity results also demand this in the present case) namely, (a) both the vacancies are present at first neighbor sites, (b) one vacancy at first-neighbor and one at second-neighbor sites, and (c) both vacancies are present at second-neighbor sites. These three possible combinations are shown in Fig. 9 by the pairs marked 1, 2, and 3,

respectively. These three cases reduce the octahedral symmetry of the crystal field to D_{2h} , C_s , or D_{4h} symmetries, respectively. The optical results in the present case can be explained on the basis of D_{2h} or C_s symmetries, but the dielectric-loss results require the postulation of an arrangement shown by the pair marked 2 (symmetry C_s). The other possible pairs cannot explain the dielectric-loss results. Hence the optical and dielectric-loss results suggest a local C_s symmetry at the ion site.

ACKNOWLEDGMENTS

The authors wish to acknowledge helpful discussions with Professor S. C. Jain, Solid State Physics Laboratory and Professor C. Ramasastry, Head of the Physics Department at the Indian Institute of Technology. The optical-absorption work at liquid-helium temperature reported in this paper was done at the Physicalisches Institute, Stuttgart by one of us (S. R. K.). The authors would like to thank Dr. H. J. Paus for considerable help in this work. One of the authors (B. D. S.) wishes to acknowledge a financial grant from CSIR in the form of Senior Research Fellowship.

- ¹J. H. Schulman and W. D. Compton, *Color Centers in Solids* (Pergamon, New York, 1962).
- ²W. B. Fowler, *Physics of Color Centers* (Academic, New York, 1968).
- ³S. Radhakrishna and B. V. R. Chowdari, *Phys. Status Solidi* **14**, 11 (1972).
- ⁴M. Chemla, *Ann. Chim. Phys.* **1**, 959 (1956).
- ⁵R. Reisfeld and A. Honigbaum, *J. Chem. Phys.* **48**, 5565 (1968).
- ⁶S. Radhakrishna and K. P. Pande, in *Proceedings of the Indo-Soviet Conference on Solid State Materials*, Bangalore, India, 1972 (unpublished).
- ⁷F. J. Keneshea and W. J. Fredericks, *J. Phys. Chem. Solids* **26**, 1787 (1965).
- ⁸S. Radhakrishna and A. M. Karguppikar, *J. Phys. Chem. Solids* **34**, 1497 (1973).
- ⁹A. B. Lindiard, *Handbuch der Physik*, edited by S. Flügge (Springer, Berlin, 1957), Vol 20, p. 246.
- ¹⁰G. H. Dieke, *Spectra and Energy Levels of Rare Earth Ions in Crystals* (Interscience, New York, 1968).
- ¹¹R. K. Asundi, R. C. Naik and P. R. Rao, *Proc. Indian Acad. Sci. A* **73**, 240 (1971).
- ¹²B. D. Sharma, Ph.D. thesis (Indian Institute of Technology, 1973) (unpublished).
- ¹³G. H. Dieke and R. Sarup, *J. Chem. Phys.* **29**, 741 (1958).
- ¹⁴E. Y. Wong, *J. Chem. Phys.* **35**, 544 (1961).
- ¹⁵E. Y. Wong, *J. Chem. Phys.* **38**, 976 (1963).
- ¹⁶E. Loh, *Phys. Rev.* **158**, 273 (1967); *Phys. Rev.* **147**, 332 (1966).
- ¹⁷D. S. McClure and Z. Kiss, *J. Chem. Phys.* **39**, 3251 (1963).
- ¹⁸J. Sugar, *J. Opt. Soc. Am.* **55**, 1058 (1965).
- ¹⁹C. K. Jørgensen, *Mol. Phys.* **5**, 271 (1962).
- ²⁰L. W. Barr and A. B. Kidiard, *Physical Chemistry, An Advanced Treatise* (Academic, New York, 1970), p. 151.
- ²¹S. C. Jain, in *A Short Course on Solid State Physics*, edited by F. C. Auluck (Thomson Press, New Delhi, 1972), Vol. 2.
- ²²D. Millotis and D. N. Yoon, *J. Phys. Chem. Solids* **30**, 1241 (1969).
- ²³M. P. Tosi and G. Airoldi, *Nuovo Cimento* **8**, 584 (1958).
- ²⁴F. Bassani and F. G. Fumi, *Nuovo Cimento* **11**, 274 (1954).
- ²⁵G. D. Watkins, *Phys. Rev.* **113**, 79 (1959); *Phys. Rev.* **113**, 91 (1959).
- ²⁶S. Radhakrishna, *Indian J. Pure Appl. Phys.* **5**, 497 (1967).
- ²⁷A. D. Franklin, *J. Res. Natl. Bur. Stand. (U. S.) A* **67**, 291 (1958).
- ²⁸Y. Haven and J. H. Van Santen, *Nuovo Cimento Suppl.* **7**, 605 (1958).
- ²⁹R. W. Dreyfus, *Phys. Rev.* **121**, 1675 (1961).
- ³⁰S. C. Jain and K. Lal, *Proc. Phys. Soc. London* **92**, 990 (1967).
- ³¹K. Lal and D. R. Pahwa, *Phys. Rev. B* **4**, 2741 (1971).
- ³²Y. Haven, *J. Chem. Phys.* **21**, 171 (1953).
- ³³J. S. Dryden and J. S. Meakins, *Disc. Faraday Soc.* **23**, 39 (1957).